Combustion and Flame 159 (2012) 870–881

Contents lists available at SciVerse ScienceDirect

Combustion and Flame

journal homepage: www.elsevier.com/locate/combustflame

Detonability of natural gas–air mixtures

Vadim N. Gamezo [b,*], R. Karl Zipf Jr. [a], Michael J. Sapko [a], Walter P. Marchewka [a], Khaled M. Mohamed [a], Elaine S. Oran [b], David A. Kessler [b], Eric S. Weiss [a], James D. Addis [a], Frank A. Karnack [a], Donald D. Sellers [a]

[a] Office of Mine Safety and Health Research (OMSHR), National Institute for Occupational Safety and Health (NIOSH), Pittsburgh, PA 15236, USA
[b] Laboratory for Computational Physics and Fluid Dynamics, Naval Research Laboratory, Washington, DC 20375, USA

ARTICLE INFO

Article history:
Received 15 April 2011
Received in revised form 9 August 2011
Accepted 10 August 2011
Available online 16 September 2011

Keywords:
Methane–air
Detonability limits
Detonation cells

ABSTRACT

Direct initiation experiments were carried out in a 105 cm diameter tube to study detonation properties and evaluate the detonability limits for mixtures of natural gas (NG) with air. The natural gas was primarily methane with 1.5–1.7% of ethane. A stoichiometric methane–oxygen mixture contained in a large plastic bag was used as a detonation initiator. Self-supporting detonations with velocities and pressures close to theoretical CJ values were observed in NG–air mixtures containing from 5.3% to 15.6% of NG at atmospheric pressure. These detonability limits are wider than previously measured in smaller channels, and close to the flammability limits. Detonation cell patterns recorded near the limits vary from large cells of the size of the tube to spiral traces of spin detonations. Away from the limits, detonation cell sizes decrease to about 20 cm for 10% NG, and are consistent with existing data for methane–air mixtures obtained in smaller channels. Observed cell patterns are very irregular, and contain secondary cell structures inside primary cells and fine structures inside spin traces.

Published by Elsevier Inc. on behalf of The Combustion Institute.

1. Introduction

This work was initiated to address safety concerns related to explosive gas mixtures that form in coal mines. These mixtures are composed of air and natural gas (NG) released from coal beds. Similar explosive mixtures may form during production, transportation, or utilization of NG. Most accidental NG explosions are deflagrations, although the worst-case scenarios involve detonations that can be extremely destructive and generate peak pressures of 10 MPa on reflections. It is, therefore, very important to know under what conditions NG–air mixtures can or cannot detonate.

1.1. Effect of natural gas composition on detonability

The composition of NG is not strictly defined and varies with source. Typically it includes 82–99% of CH_4 by volume depending on the gas origin [1,2], as well as ethane, propane, and small amounts of higher hydrocarbons. A few percent of nitrogen and CO_2 can also be present. A typical coalbed gas (often called coalbed methane) is usually mostly CH_4 with less than 2% of ethane and heavier hydrocarbons, but sometimes it may contain up to 15% of CO_2 [3,4].

The variability of NG composition results in large uncertainties in explosive properties of NG–air mixtures. It has been shown, for example, that small additives of ethane, propane, and higher alkanes significantly decrease ignition delays in CH_4–O_2 and CH_4–air mixtures [5,1,2]. The induction length δ of a ZND detonation in stoichiometric methane–ethane–air mixtures computed in Ref. [5] can be approximated as

$$\delta/\delta_0 = 1 - 13.52x + 167.5x^2 - 1370x^3 + 5846x^4 - 9625x^5 \qquad (1)$$

where $\delta_0 = 2.41$ cm is the induction length for CH_4–air, and $x \leqslant 0.2$ is the volume fraction of ethane in the methane–ethane mixture. According to this equation, 8% ethane in NG decreases the induction length by a factor of 2.

Ignition delays usually correlate with both the energy required for detonation initiation and the detonation cell size, both of which characterize the detonability of the mixture. Thus, the detonability of NG–air varies with NG composition and can differ significantly from that of CH_4–air. For example, ethane has a strong effect on the initiation energy of stoichiometric methane–ethane–air mixtures [6]. When the ethane concentration in the methane–ethane mixture is decreased from 30% to 10% by volume, the minimum energy required for detonation initiation in cylindrical geometry increased exponentially from 12.5 kJ/cm to 25 kJ/cm. A rough extrapolation to lower ethane concentrations shows that the initiation energy may increase by two orders of magnitude for pure CH_4–air. A similar extrapolation of experimental results [7] obtained for CH_4–O_2–N_2 mixtures using the same experimental setup gives the initiation energy for CH_4–air around 7.5 MJ/cm. Both of these extrapolations are far-fetched and could be easily wrong by

* Corresponding author. Fax: +1 202 767 4798.
E-mail address: gamezo@lcp.nrl.navy.mil (V.N. Gamezo).

0010-2180/$ - see front matter Published by Elsevier Inc. on behalf of The Combustion Institute.
doi:10.1016/j.combustflame.2011.08.009

an order of magnitude, but they do show that the NG composition can drastically change the detonability of NG–air mixtures.

In this paper, we use the word "methane" or the chemical formula CH_4 when we discuss pure methane. In some cases, the word "methane" is also used to describe gas mixtures composed mostly of CH_4. For example, we sometimes refer to NG–air mixtures used in our experiments as methane–air mixtures, because the NG we used was primarily CH_4 with only 1.5–1.7% of ethane and trace amounts of higher hydrocarbons. We should note, however, that according to Eq. (1), 1.5–1.7% of ethane in NG decreases the induction delay by a factor of 0.8 compared to that in CH_4–air.

1.2. Prior studies of detonability of methane–air and NG–air mixtures

Because of the stability of the methane molecule, CH_4–air is the most insensitive hydrocarbon–air mixture with respect to the detonation initiation. There are still no confirmed reports of successful initiation of self-supported detonations in unconfined NG–air or methane–air mixtures.

An early report [8] claimed a detonation initiation using 1 kg of TNT inside a 3 m rubber sphere filled with a stoichiometric methane–air mixture. The observed detonation velocity was 1540 m/s, which is well below the calculated Chapman–Jouguet velocity D_{CJ} = 1815 m/s. These results were analyzed in Ref. [9] with a conclusion that the observed detonation was most likely decaying. There is also some uncertainty in the exact mixture composition, since the purity of methane used in the experiments [8] is not specified.

Another report [10] describes "erratic, uneven detonations" initiated in a 1.2 × 1.2 × 6 m plastic bags filled with NG–air mixtures by 1 kg of high explosive. The NG used in these experiments contained 2.5% of ethane. Plastic bags were supported by a steel pipe frame. Unsteady detonation regimes with velocities 1195–1325 m/s were observed only for NG concentrations 8.6–8.8%. Tested mixture concentrations ranged from 5.2% to 12.5%, including the stoichiometric 9.5% mixture, which did not detonate. The authors suggest that observed "poorly defined" detonation fronts were partially supported by reflections from the steel frame structure.

Extrapolation of experimental results [9] obtained for various methane–O_2–N_2 mixtures suggests that detonation initiation in unconfined methane–air would require about 22 kg of tetryl. Large-scale experiments [11] have shown that 37 kg of Composition B did not initiate a detonation in a stoichiometric (9.5%) methane–air in a hemispherical geometry.

There are only three published works in which high explosives were used to initiate methane–air detonations in tubes. Early experiments [12] carried out at the Bureau of Mines Experiment Station in Pittsburgh have shown that 50 g of a high explosive (65% ammonium nitrate/14.6% TNT/20.3% sodium chloride) initiate a detonation-like wave inside a 30.5 cm diameter tube filled with a 9.1% methane–air mixture. The wave velocity measured in the 3.65 m long tube varied between 1820 and 1950 m/s, which is slightly higher than the calculated D_{CJ} = 1801 m/s. The authors conclude that the observed regime is not a "true" detonation, but a transitional regime partially supported by the energy of the initiator.

A longer, 11.2 m tube with the same 30.5 cm diameter was used in experiments [13] in which detonations were initiated using 50 g and 70 g of a slightly more powerful high explosive (50% ammonium nitrate/50% TNT). The detonation propagation was observed using multiple optical windows, from which the author concluded that steady-state detonations are possible for mixtures containing from 6.3% to 13.5% of methane. The methane used in these experiments was, in fact, a natural gas that contained ~2% of higher hydrocarbons.

A larger, 13.1 m long and 43 cm diameter tube was used in Ref. [14] to measure detonation cells in hydrocarbon–air mixtures including methane (99.99% pure). Detonations in various mixtures were initiated with a planar charge of Detasheet high explosive. Authors say that typically 40 g of the explosive were used, but they do not indicate if this was enough for the stoichiometric methane–air mixture.

The difficulties encountered in initiating self-supporting detonations in methane–air using high explosives may create the perception that methane–air mixtures can only detonate under extraordinary circumstances not seen in the practical world. A number of experiments with different ways of detonation initiation have shown that this perception is wrong. Detonations in methane–air have been ignited in confined conditions using booster detonations in more sensitive gas mixtures [15,16] or deflagration-to-detonation transition (DDT) in smooth [17,18] or obstructed [19–22] channels. Still, the available experimental data on detonations in methane–air mixtures are very limited because detonation experiments using these mixtures usually require large facilities. Ideally, a detonation tube should be wide enough to fit several detonation cells, and the tube length should be sufficient to observe a self-supporting quasi-steady-state detonation.

Detonation cell sizes measured in a 183 cm diameter tube [16] for 9.6% methane–air mixture are about 28 cm. Cell sizes reported in Ref. [14] for a 43 cm diameter tube and 9.5% methane–air mixture are 30.5 ± 15.3 cm. Cell sizes measured in a 52 cm diameter tube [20] are 21 ± 8 cm for the stoichiometric mixture, and these can increase to the tube width for lean (8.5%) and rich (12%) mixtures. The wide range of measured cell sizes reflects the fact that cellular structures in methane–air are very irregular.

In smaller tubes, methane–air detonations can only propagate in the spinning mode. This mode was initiated in a 6.35 cm wide square tube by a hydrogen–oxygen booster to determine initiation energies for methane–air mixtures of different concentrations [15]. A minimum initiation energy of 9 MJ/m^2 has been obtained for 11% methane. Lower and upper detonability limits determined for methane–air in the same experiments are 8% and 14.5% methane. The smallest tube diameter in which a methane–air detonation was ever observed is 3.6 cm [21]. Detonability limits reported in Ref. [21] for a 5 cm diameter tube are 7.5% and 11.5%.

In this paper, we study the detonability of NG–air mixtures in a 105 cm diameter tube using a CH_4–oxygen mixture in a bag as an initiator. We determine detonability limits, record detonation cell patterns for the full range of NG concentrations, and measure detonation velocities and pressures.

2. Test facility

Experiments were carried out at the Gas Explosion Test Facility (GETF) at NIOSH Lake Lynn Laboratory (LLL). The facility consists of the detonation tube, supporting systems for gas injection, mixing, sampling and analysis, the ignition system, the diagnostic equipment, and a remote control system. Pictures of the facility are shown in Fig. 1, and schematic diagrams are shown in Fig. 2.

2.1. Detonation tube

The tube is located in the upper quarry of LLL. It is fabricated from sections of hot-rolled steel pipe that have been welded together. The total length of the tube is 73 m, and the internal diameter is 105 cm. The straight tube rests in a plane on 18 equally spaced concrete blocks weighing about 1.8 t each, and is attached to these blocks with 9.5 mm galvanized steel cable. The tube has an inclination of about 2°, with the open end about 2.5 m higher than the closed end.

Fig. 1. Gas Explosion Test Facility (GETF) at NIOSH Lake Lynn Laboratory. Views from the open (a) and closed (b) ends.

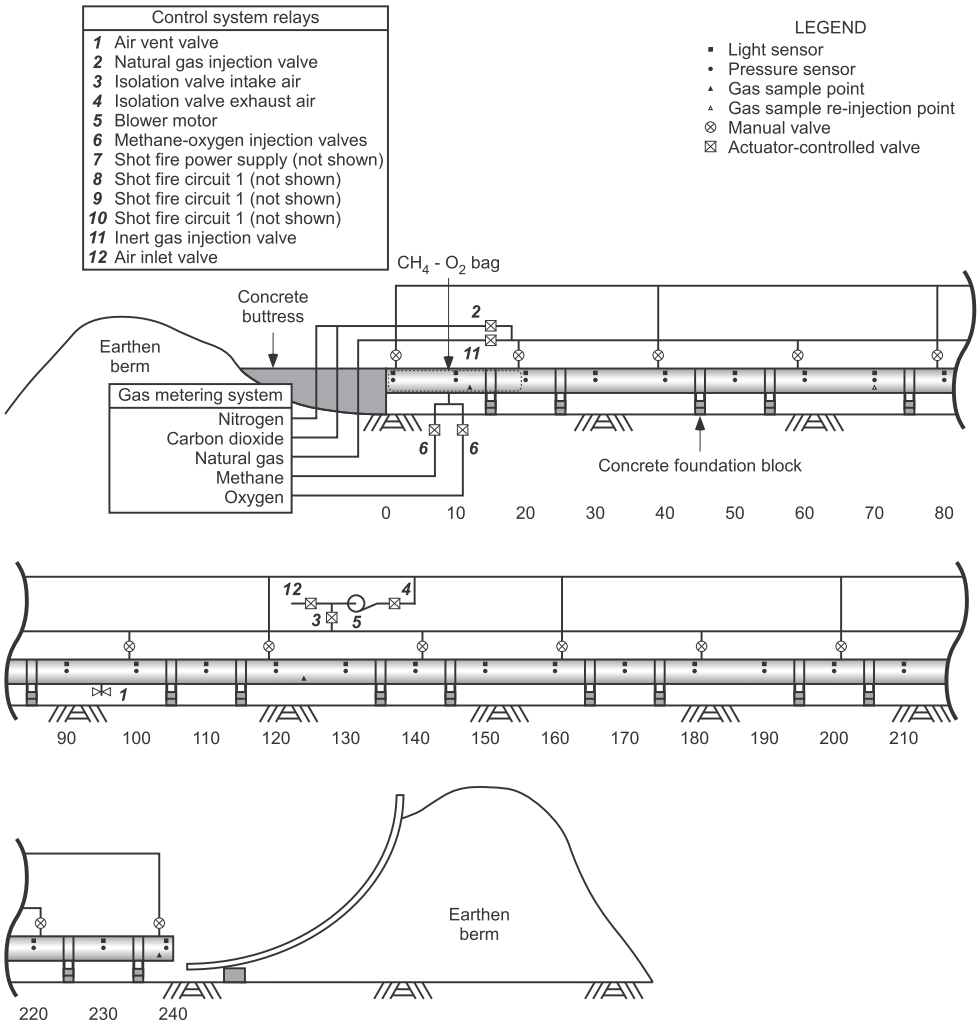

Fig. 2. GETF schematics.

The closed end is permanently sealed with a 12.7 mm welded steel plate. It rests against a 14 t concrete block poured between the tube and a 5-m high earthen berm, as shown in Fig. 1a. The total weight of the pipe, concrete supports, and the earthen berm that resists the tube recoil is at least 175 t. The open end of the tube is located about 15 m from the 20-m high quarry wall. A 15 t concave ramp deflector fabricated from curved steel H-beams is installed at about 2 m from the open end, leaning against another berm. The deflector is designed to direct shock waves exiting the tube upward into the atmosphere in order to prevent damage to nearby structures due to reflections of strong shocks from the quarry walls.

The steel pipe has a wall thickness of 9.5 mm, minimum yield strength of 248 MPa, and an ultimate tensile strength of 414 MPa. For stoichiometric CH_4–air mixtures, the quasi-static CJ detonation wave pressure is 1.66 MPa, and that pressure could persist

for time periods longer than 0.1 s. Based on hoop stress calculations with this quasi-static pressure, the safety factor against deformation is about 2.70, and the safety factor against rupture is 4.50. Higher pressure pulses with shorter durations affect the tube walls in the vicinity of the detonation front, during shock reflections, and during the detonation initiation. The highest peak pressure recorded so far at GETF is about 7 MPa, and the tube shows no evidence of deformation or damage.

2.2. Gas mixing and analysis

A very important part of GETF is the gas mixing system that enables creation of homogeneous NG–air test mixtures inside the tube with predefined equivalence ratios. The mixing system consists of an enclosed blower fan, an intake manifold, and an exhaust manifold. The 2.25 kW blower fan delivers 26.5 m^3/min operating at 27.2 cm of water static pressure. Manifolds are made with 10 cm diameter pipe, and are connected to the detonation tube through 7.5 cm inlet and outlet riser pipes. The riser pipes are equipped with manual ball valves that can be used to balance the flow from each inlet and outlet; in these experiments, however, all the valves were open. There are also two remotely operated ball valves between the blower fan and manifolds. These are open during the mixing process, and closed before ignition to protect the fan.

Prior to filling the explosion tube with the amount of NG that produces the desired test mixture composition, a 20 cm diameter access port near the closed end of the tube is opened, and the tube is ventilated for at least 30 min using a portable fan. The blower fan is also operating at this time. This ensures that the tube and the mixing system are filled with fresh ambient air. Then the portable fan is removed, the access port is closed, and a 0.15-mm thick plastic diaphragm is placed over the open end of the tube. Natural gas is introduced into the intake manifold at the beginning of the mixing process.

As shown in the schematic in Fig. 2, the intake manifold has six evenly spaced inlets: three are on each side of the blower fan. The exhaust manifold has seven outlets: three are on one side of the blower fan and four on the other. The first riser pipe, located about 1 m from the closed end of the tube, is an outlet. That is gas flows out of the manifold into the tube. The second riser is an inlet in which gas flows into the manifold from the tube. The third riser is an outlet, the fourth riser is an inlet, and so on. The last riser, located 82 cm from the open end, is an outlet.

When the blower fan operates, the gas mixture in the tube is drawn into the inlet risers, through the intake manifold, through the blower, through the exhaust manifold, and then re-injected trough the outlet risers. Since both inlets and outlets are distributed along the length of the detonation tube, the system has multiple recirculation circuits that merge in the intake manifold and split in the exhaust manifold, thus providing efficient gas mixing. The volume of the detonation tube is 63.4 m^3. The 2.25 kW blower fan moves 26.5 m^3/min, and thus the air exchange time is less than 3 min. To achieve a homogeneous test mixture, typical mixing times range from 30 to 45 min.

A sample draw system enables remote collection and analysis of samples of the test mixture. During gas mixing, samples are drawn continuously from the closed end, middle, and open end of the tube to an infrared gas analyzer (Siemens Ultramat 23) located about 300 m away from the detonation tube in the control building. Collected samples are then returned to the detonation tube through a re-injection line, except for a small portion passing through the gas analyzer. The sample draw system provides real-time gas concentrations at three different locations along the tube and assures homogeneity of the test mixture.

The mixture composition in the tube is controlled in three different ways. First, a pre-calculated amount of natural gas is injected into the tube using a conventional natural gas meter (Sensus 135 S-275). Second, gas samples are analyzed with the remote infrared gas analyzer during mixing. Finally, two samples of the gas mixture are drawn after the mixing is completed and analyzed later, off-site, using gas chromatography. In most experiments with this detonation tube, the desired concentration of natural gas in the test mixture was created with the accuracy ±0.2% by volume.

2.3. Ignition

To ignite a detonation in the NG–air test mixture, a large plastic bag filled with a stoichiometric methane–oxygen mixture is placed at the closed end of the tube. The cylindrical bag has a diameter of about 1 m, and is made of 0.15 mm plastic film. The bag volume typically varies between 2.9 m^3 and 5.8 m^3 from one series of experiments to another. Smaller bags, 1.44 and 0.72 m^3, were also used in a few experiments to test the effect of the ignition energy.

To inflate the bag, separate methane and oxygen tanks are used to meter pre-calculated amounts of each gas, which flows through orifices into the bag. Gas was administered through separate lines with check valves and flash back arrestors in each line. The bag is inflated remotely after NG–air mixing in the tube is complete. The excess mixture in the tube displaced by the inflating bag is released into atmosphere though one of the gas sampling ports.

Detonation in the stoichiometric methane–oxygen mixture is initiated with a non-electric #8 blasting cap containing about 0.45 g pentaerythritol tetranitrate (PETN) placed at about 0.5 m from the closed end of the tube. The methane–oxygen mixture has a detonation cell size of 2–3 mm, propagates with a velocity close to D_{CJ} = 2490 m/s, burns all the mixture in the bag, and generates a strong shock in the tube. This shock may or may not ignite a detonation in the NG–air test mixture, depending on the mixture composition and the size of the igniter bag.

2.4. Diagnostics

The tube is equipped with 23 quartz-piezoelectric-type pressure transducers and 23 light sensors placed in pairs (pressure + light) approximately every 3 m on the tube wall, as shown in Fig. 2. The sensors are connected to two separate 24-channel data acquisition units, one of which records all pressure signals, another records all light signals, and both units also record a synchronization signal from a signal generator.

The light sensors are silicon phototransistors (Optek NPN OP800WSL) with a rise time of about 2 μs and a spectral response from 600 to 1100 nm. Sensors are mounted at the end of a small tube that is 15 cm long with an inside diameter of 0.32 cm. The field of view for the light sensor is about 5 cm on the opposite side of the 105-cm diameter detonation tube.

The piezoelectric pressure sensors (PCB Piezotronics CA102B04) have a range of 0–6900 kPa and 1 μs rise time. For most of the experiments reported here, the pressure sensors were threaded directly into side wall of the detonation tube, and recorded wall vibrations prior to the arrival of the detonation wave. These records show that the vibrations propagate along the tube at about 5200 m/s, which is close to the estimate for the longitudinal wave velocity $\sqrt{E/\rho} = 5044$ m/s in a mild steel based on the Young's modulus E = 200 GPa and the density ρ = 7860 kg/m^3.

The tube wall vibrations cause pressure signal oscillations with the amplitude up to 0.4 MPa, as shown in Fig. 3, line a. These oscillations do not prevent detection of strong detonation shocks relevant for this work. Nevertheless, some efforts were made to reduce precursor oscillations that could impede analysis of other GETF

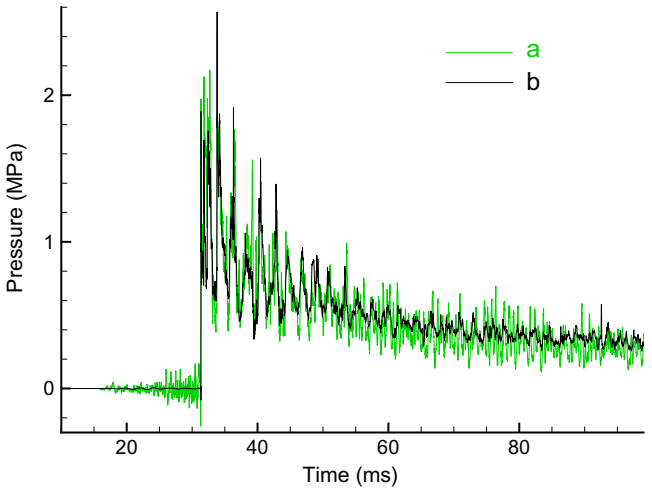

Fig. 3. Typical signals produced by pressure sensors without (a) and with (b) anti-vibration support. Test #41, 5.9% NG.

experiments involving weaker shocks. These oscillations practically disappeared (Fig. 3, line b) when pressure sensors were decoupled from the tube using double-studded silicone gel anti-vibration mounts, as shown in Fig. 4.

The data acquisition system consists of two separate 24-channel units (National Instruments CompactRIO) with a sampling frequency 50 kHz. This frequency limits the time resolution for all recorded signals to 20 μs. The time error between two signals generated by a wave propagating between two sensors located 3 m apart can reach 40 μs. For the detonation velocity 1800 m/s, the uncertainty in position of the detonation wave is 0.072 m in 3 m or 2.4%. Therefore, the uncertainty in the measured detonation velocity is also 2.4% or ±43 m/s. If the velocity is constant, the uncertainty is significantly reduced using multiple sensors at greater distances apart.

Before each experiment, two smoke foils are placed between 0.15 and 2.8 m from the open end of the tube. The 1.2-m × 1.2-m foils are made of 1.6-mm thick aluminum sheets rolled to a 0.5-m radius of curvature. They are secured to the inside top of the tube with bolts around the perimeter of the foils. The upstream edge of each foil is inserted into a welded metal slot. Foils are covered with soot produced by acetone flames.

2.5. Remote control system

Starting from the injection of NG into the detonation tube, all operations necessary for preparing and conducting experiments are controlled remotely from the LLL control building located about 300 m away from the tube. Firing the primary ignition circuit triggers the data acquisition system. In case the primary circuit fails to ignite the methane–oxygen bag and the test mixture, two additional independent ignition circuits are available to ignite the flammable mixture using electric matches. It is also possible to vent the test mixture to the atmosphere using the gas mixing system.

3. Experimental results

Experiments reported here were conducted at GETF to determine the detonation characteristics of various NG–air mixtures containing from 4% to 19% of NG. Each experiment attempted direct initiation of detonation in the test mixture using a methane–oxygen mixture in a bag as an initiator. Detonations were observed in mixtures containing from 5.3% to 15.6% of NG. Some of the experiments produced deflagrations or shocks without combustion. Deflagration-to-detonation transition in the middle of the tube was detected in one test. Experimental conditions and results for each test are listed in Table 1.

The diagnostic equipment used in these experiments consisted of pressure and light sensors placed in pairs every 3 m on the tube wall, and smoke foils placed near the open end of the tube. Detonations were identified using four methods: (1) comparison of measured flame and shock velocities to computed D_{CJ} values; (2) comparison of recorded pressures to computed pressure profiles for ZND detonations; (3) measurement of the separation between the shock and the flame using the time difference between pressure and light signals recorded at the same location; and (4) analysis of patterns produced on smoke foils.

3.1. Pressure and light signals

Figure 5 shows typical signals produced by detonations in tests with 7.3%, 10.2%, and 14.0% NG in air, corresponding to fuel-lean, near-stoichiometric, and fuel-rich mixtures, respectively. As the detonation front arrives, the pressure rises sharply, then drops to about P_{CJ}, and then decreases slowly. Some signals show two or even three sharp peaks associated with transverse waves behind the cellular detonation front. Subsequent signal oscillations are mostly due to residual pressure waves reflecting from tube walls far behind the leading shock.

For an idealized ZND detonation, the pressure peaks at $P_{ZND} \approx 2P_{CJ}$ at the leading shock and drops to P_{CJ} at the end of the reaction zone. For the stoichiometric CH_4–air mixture, the idealized reaction-zone length is close to the ZND induction length 2.76 cm computed in Ref. [14]. For the detonation velocity in this mixture ~1800 m/s, a stationary sensor would record a pressure drop from P_{ZND} at the leading shock to P_{CJ} at the end of the reaction zone in about 15 μs.

Since the data acquisition system in GETF experiments limits the time resolution for all signals to 20 μs, the ZND reaction zone would not be resolved. For a real multidimensional unstable

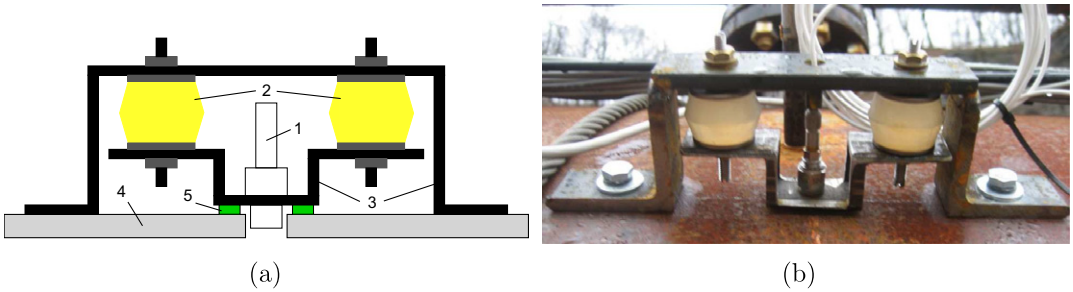

Fig. 4. Anti-vibration support for reducing precursor pressure oscillations. Schematics (a) and photo (b). 1 – Pressure sensor. 2 – Double-studded silicone gel anti-vibration mounts. 3 – Steel brackets. 4 – Tube wall. 5 – Rubber gasket (replaced after each test).

Table 1
Experiments on direct initiation of detonations in NG–air mixtures conducted at GETF. Tube diameter 105 cm.

Test	% NG	V_B (m^3)	D_S (m/s)	D_F (m/s)	P (MPa)	Cell size (cm)	Combustion mode
#61	12.42	2.89	1797	1799	1.6	64	Detonation
#59	15.67	2.89	779	-	0.2	-	No combustion
#58	15.65	2.89	786	-	0.2	-	No combustion
#57	5.31	2.89	1512	1518	1.2	Spin	Detonation
#56	16.57	2.89	783	-	0.2	-	No combustion
#55	5.37	2.89	1540	1533	1.2	Spin, max	Detonation
#54	4.94	2.66	787	-	0.2	-	No combustion
#51	5.46	2.89	1563	1558	1.2	Max	Detonation
#50	5.66	2.89	1575	1592	1.2	Max	Detonation
#49	15.53	2.89	1692	1699	1.5	Spin	Detonation
#48	6.20	2.89	1589	1583	1.4	80, max	Detonation
#47	10.39	0.722	1817	1812	–	21	Detonation
#46	10.21	1.44	1813	1826	1.6	28	Detonation
#45	10.29	2.89	1863	1860	1.6	25	Detonation
#43	17.09	5.78	832	-	0.6	—	No combustion
#42	15.63	5.78	1705	1722	1.6	62, max	Detonation
#41	5.98	5.78	1567	1570	1.4	Max	Detonation
#40	15.55	5.78	1743	1740	1.5	Max	Detonation
#39	9.97	2.89	1821	1823	1.6	21	Detonation
#38	8.52	2.89	1774	1777	1.7	39	Detonation
#37	15.32	2.89	695	–	0.3	-	Deflagration
#36	13.95	2.89	1756	1760	1.55	61	Detonation
#35	13.41	2.89	1789	1794	1.6	52	Detonation
#34	12.19	2.89	1815	1816	1.65	47	Detonation
#33	11.21	2.89	1828	1822	1.7	26	Detonation
#32	16.40	2.89	703	-	0.3	-	No combustion
#31	9.29	2.89	1799	1800	1.6	35	Detonation
#30	6.25	2.89	819	–	0.5	-	Deflagration
#29	7.30	2.89	1689	1687	1.5	55	Detonation
#27	10.17	2.89	1831	1873	1.5	25	Detonation
#26	19.06	2.89	747	-	0.3	—	No combustion
#24	4.26	3.26	512	-	0.1	—	No combustion
#22	14.87	3.26	1810	1794	1.6	—	Detonation
#21	13.89	3.26	1769	1717	1.6	—	Detonation
#20	10.37	3.26	1804	–	1.5	—	Detonation
#19	9.61	3.26	1805	1842	1.5	—	Detonation
#18	7.16	3.26	1691	–	1.7	—	DDT at 39 m
#17	6.25	3.26	1570	1584	1.4	—	Detonation

V_B is volume of booster bag, D_S is average shock velocity, D_F is average flame speed, P is pressure measured behind the main peak. For Test #18, average shock velocity is 943 m/s before DDT and 1691 m/s after DDT.
"Max" – one large cell of the size of the tube, "spin" – spiral trace of spin detonation, "—" smoke foil is not installed, "–" not measured, "-" not applicable.

detonation wave, however, the leading shock contains weak and strong parts that locally propagate with velocities below and above D_{CJ}. For strong parts, the reaction zone in GETF experiments is not resolved. Recorded peak pressures are not necessarily the maximum pressures to which the sensor is exposed. For weak parts, the reaction-zone length, determined from the post-shock temperature and chemical kinetics, can be very large. In reality this means that the reaction front decouples from weak parts of the leading shock, and the distance between the shock and the flame depends on the dynamics of transverse shock waves. This distance can be resolved in GETF experiments using a combination of both pressure and light sensors.

Pressure and light signals recorded at selected locations in a Test #39 with 10.0% NG in air are shows in Fig. 6a. The sensitivity of light sensors was tuned to show a strong rise of the signal when hot combustion products cross the line of sight of the sensor. In several tests, ion probes were installed on the tube wall next to selected light sensors to check the sensor calibration. For example, the ion probe signal and the light signal shown in Fig. 6a for 27.28 m rise practically the same time. The difference of 20–30 μs is very close to the time resolution (20 μs) of the data acquisition system.

The detonation in the near-stoichiometric mixture used in Test #39 produces light signals that rise at the leading shock or slightly behind with typical delays of 0–40 μs. For the detonation velocity ~1800 m/s, this corresponds to a distance of 0–7 cm between the shock and the flame. This is consistent with the structure of a detonation front with the cell size 20–30 cm measured for 10% NG (see below).

Far from stoichiometric conditions, detonation cells grow and the maximum possible gap between the leading shock and the flame increases. Figure 6b shows selected pressure and light signals recorded near the detonability limit (Test #57, 5.3% NG). In this case, the shock and the flame are coupled in some locations, and decoupled in others. Delays between the leading shock and the flame arrival vary within the range 0–300 μs, which corresponds to the distance 0–45 cm between the shock and the flame. The maximum observed distance of 45 cm, almost a half of the tube diameter, is too large even for the detonation cell size comparable to the size of the tube. In this test, the detonation propagates in a spinning mode, as discussed below.

All pressure and light signals for Tests #39 and #57 are summarized in x–t diagrams in Fig. 7. These diagrams show that the shock velocity remains practically constant from the beginning to the end of the tube. For many other tests with a successful detonation initiation, the shock velocity measured between the first two sensors at 2.9 and 5.9 m is higher, above 2000 m/s. This is consistent with an overdriven detonation resulting from the ignition by the stoichiometric methane–oxygen mixture (D_{CJ} = 2490 m/s) in a bag, which is usually 3.3–6.7 m long.

The results of direct initiation experiments are summarized in Fig. 8, which shows measured shock and flame velocities as func-

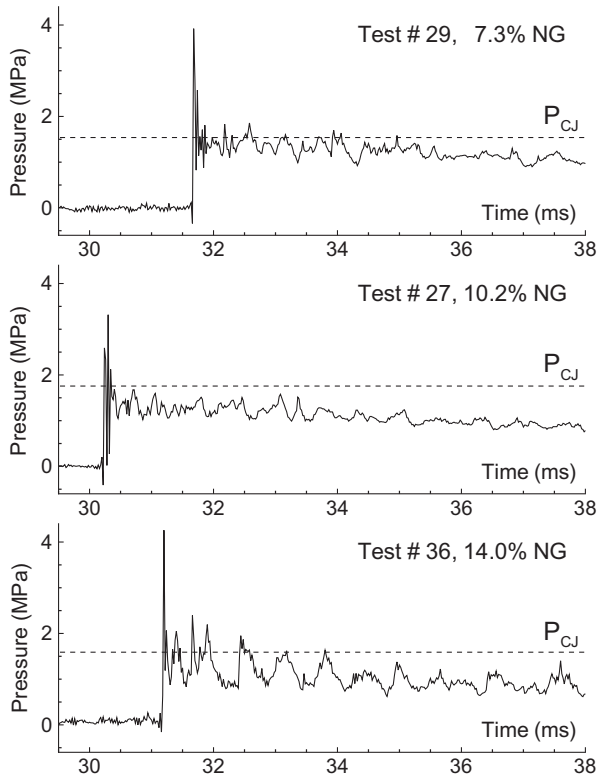

Fig. 5. Typical pressure signals produced by detonations for 7.3, 10.2, and 14.0% NG in air (Tests #29, #27, #36). Dashed line shows computed CJ pressure. All signals are recorded by the same sensor located at 42.39 m from the closed end of the tube.

tions of NG concentration. The theoretical CJ detonation velocity [23] is also included in Fig. 8 as a solid line. Detonation in the test mixture is sustainable for NG concentrations from ~5.3% to ~15.6% by volume. The difference between the measured and theoretical detonation velocities is less than 50 m/s or 3%. When the detonation initiation was unsuccessful, the shock velocity decreased to 500–800 m/s for lean mixtures, and to 700–800 m/s for rich mixtures. Test mixtures with less than 4.9% or more than 16.0% of NG did not sustain either a detonation or a deflagration in these experiments.

Figure 9 shows the measured detonation pressure a function of NG concentration. The theoretical CJ detonation pressure is also included as a solid line. Again, there is good agreement between measured and theoretical values, considering that the estimates of the detonation pressure behind the main shock are ±0.3 MPa. The maximum CJ pressure, 1.77 MPa, occurs for ~10% NG, and declines as the lower and upper limits are approached. Even at the limits of 5.3% and 15.6%, CJ pressures are still high at about 1.2 MPa and 1.5 MPa, respectively. Thus, NG–air mixtures develop substantial pressures over the entire detonable range.

3.2. Detonation cells

Figure 10 shows the measured detonation cell size as a function of mixture composition. Tests for mixture compositions in the range 5.3–15.6% NG produced cell patterns, and those outside the range did not. The number of cells in a foil ranged from 1 to 8, depending on the mixture. The minimum average cell size 20–30 cm was observed for slightly rich mixtures with 10–11% NG. The maximum average cell size recorded for mixtures with 7–14% NG was 55–65 cm. The variability of the cell measurements is on the order of 30% due to the irregularity of the cell patterns.

Several tests near the detonability limits produced large cells comparable to the size of the tube. To our best knowledge, these are the largest detonation cells ever recorded in experiments. For example, Test #40 with a 15.6% mixture resulted in one large cell that spread over two smoke foils to the total length of 170 cm. The cell width in this case can be considered as the tube diameter d = 105 cm, or the half-circumference $0.5\pi d$ = 165 cm. The latter assumes a double-head spin detonation characterized by two triple points that propagate along the wall in opposite circumferential directions. All points shown in Fig. 10 at 165 cm correspond to one large cell of the size of the tube. In some cases, smaller cells were also observed, and this is shown by error bars extending down from 165 cm.

Three tests near the limits (#49, 15.5%, #55, 5.3%, and #57, 5.3%), produced spiral traces of single-head spin detonations. These points are shown in Fig. 10 for the equivalent cell size πd = 330 cm [22]. One of these tests (#55) produced a spiral trace in one foil, and a large cell in the other foil. This is shown by two points, at 330 and 165 cm connected by a vertical bar.

Figure 10 also includes experimental data [20,14,16] and the computed curve based on a model [24]. There is reasonable agreement between the measured and theoretical cell sizes, considering the high variability of the cell sizes measured for each experiment.

Cell patterns left on smoke foils by developed detonations in GETF experiments are very irregular. Examples of these patterns are shown in Fig. 11. In addition to the large primary cells that vary in size and shape, there are also secondary cell structures inside primary cells. These secondary cells can be 1–3 orders of magnitude smaller than the primary cell. For example, Fig. 12a shows small, relatively regular cells inside a large, 80 cm wide primary cell. This kind of secondary cell structures is typical of systems with high activation energies [25–27], though multi-level cell structures can also form when the energy release in a detonation wave occurs in multiple stages on different time scales [28–32].

Another example in Fig. 12b shows irregular secondary structures observed around the point of collision of two triple points for 5.5% mixture. The primary cell in this case is about the size of the tube and is probably produced by a double-head spin detonation. Further decrease of NG concentration leads to a single-head spin (or simply spin) detonations.

Spin detonations observed near the detonability limits produce characteristic spiral traces as shown in Fig. 13. These traces can be regular (a) or irregular (b). The spin detonation regime occurs when the natural detonation cell size becomes larger than the tube diameter, and the cellular front structure degenerates to one triple-shock configuration that propagates along the tube wall [33]. The transverse wave in this configuration is a detonation that can be unstable and produce a fine cell structure inside the spiral trace, as shown in Fig. 14.

These fine cell structures are most visible for spin regimes, but sometimes we also see them inside wide boundaries of large primary cells. In both cases, fine structures are due to the instability of transverse detonations in systems with high activation energies. They were previously observed in experiments with spin detonations [34–36] and in numerical simulations [27,37].

Since transverse detonations propagate in the gas, which is already compressed by the leading shock, they develop very high pressures. This high pressure produced a deformation of the smoke foil along the spin trace shown in Figs. 13b and 14b. The deformation cannot be seen in the photo, but a visual analysis of the actual foil clearly shows ~1 mm deep groove along the trace.

All pressure signals recorded in Test #57 starting from 12 m (Fig. 7b) show multiple strong pressure oscillations with a period 2.1 ms, which is significantly longer than the dominant period of 0.6 ms observed in experiments for near-stoichiometric mixtures (Fig. 7a). If we relate these oscillations to the rotation of the spin

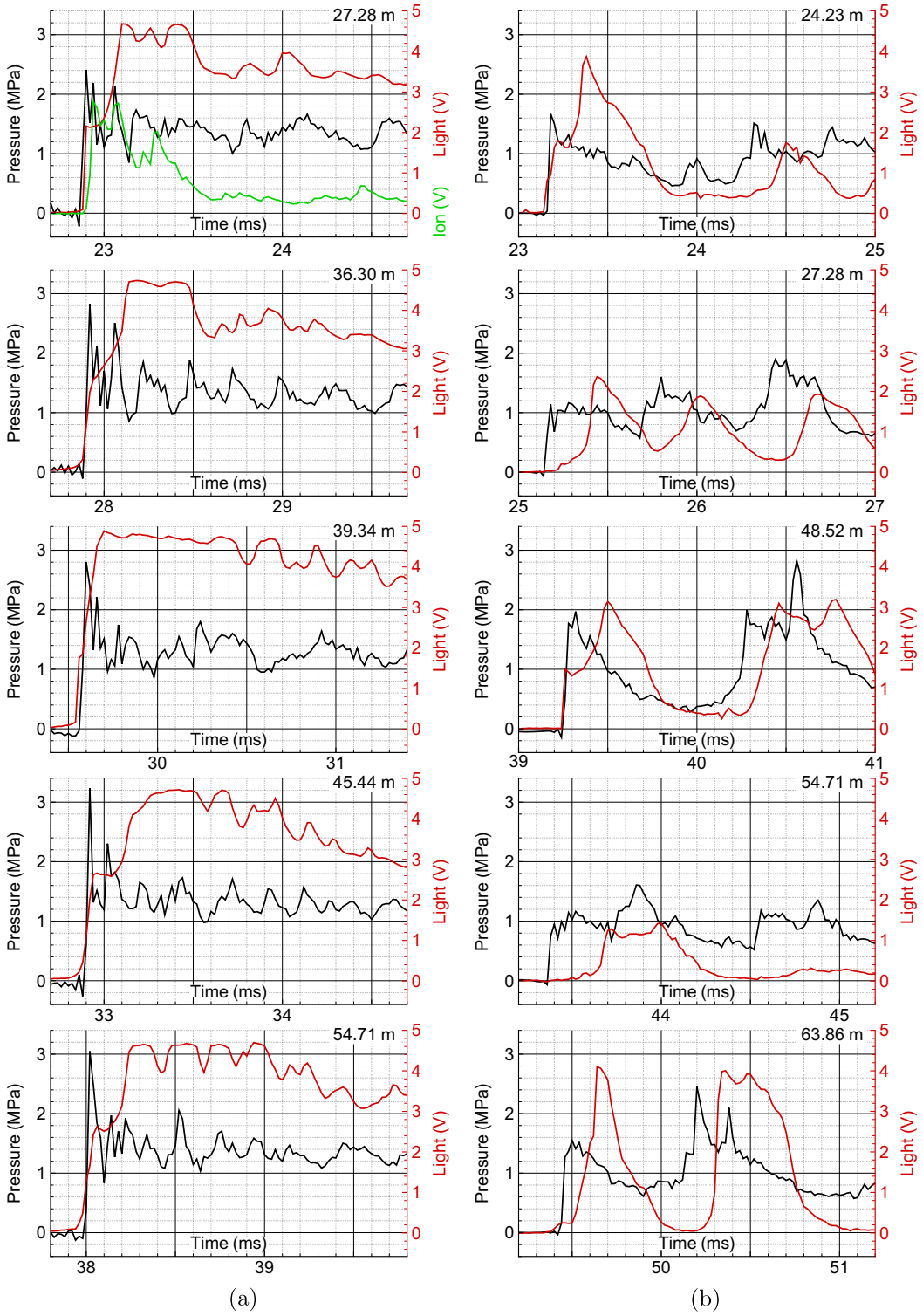

Fig. 6. Pressure (black) and light (red) signals recorded at selected locations for (a) Test #39, 10.0% NG and (b) Test #57, 5.3% NG. Green line shows ion probe signal. Sensor locations are indicated in top right corner of each frame. (For interpretation of the references to color in this figure legend, the reader is referred to the web version of this article.)

head, the rotation period of 2.1 ms gives the transverse wave speed $1.05\pi/0.0021 = 1571$ m/s. Since the leading shock velocity in this experiment is 1512 m/s, the angle of the resulting spiral trajectory of the transverse wave should be close to 45°, which is approximately the angle observed in Fig. 14. This confirms the spin detonation regime in Test #57 and shows that detonation propagates in this regime for the most part of the tube length.

4. Discussion and conclusions

The most important practical result of these experiments is the new extended range of detonability for methane–air mixtures observed for the first time in a large, 105 cm diameter tube. The new range, 5.3–15.6%, almost encompasses the entire flammability limits of 5–16% methane in air, as reported in Ref. [38].

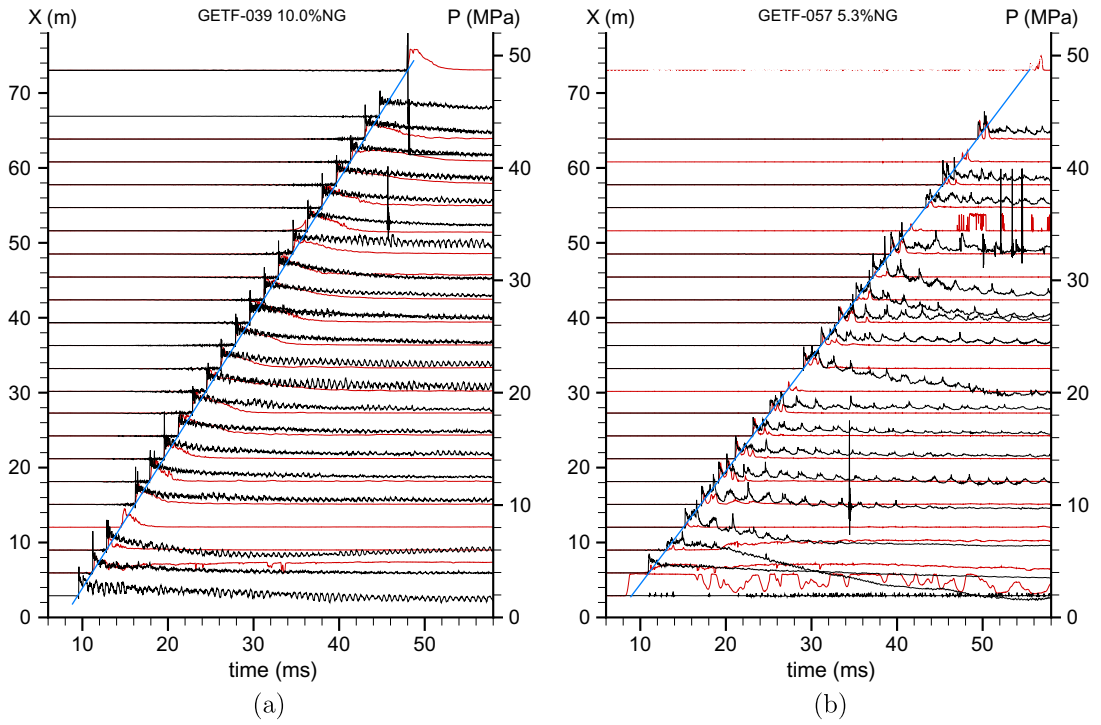

Fig. 7. The x–t diagrams summarizing all pressure (black) and light (red) signals for (a) Test #39, 10.0% NG and (b) Test #57, 5.3% NG. Blue lines correspond to constant shock speeds (a) 1820 m/s and (b) 1512 m/s. (For interpretation of the references to color in this figure legend, the reader is referred to the web version of this article.)

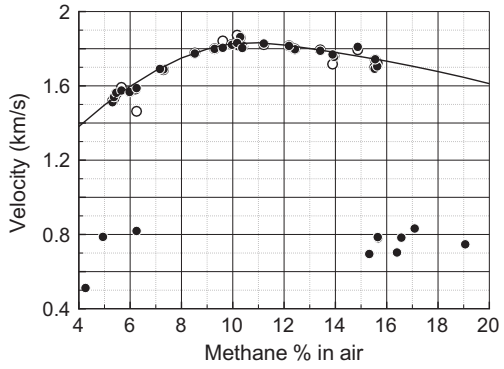

Fig. 8. Average shock and flame velocities (black and white points, respectively) measured in direct initiation experiments as a function of mixture composition. Solid line shows computed CJ velocity.

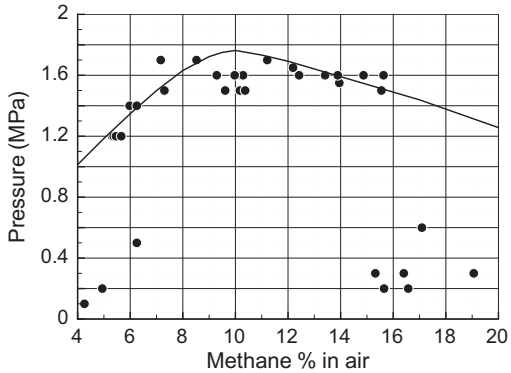

Fig. 9. Pressure measured behind the main peak in direct initiation experiments (points) as a function of mixture composition. Solid line shows computed CJ pressure.

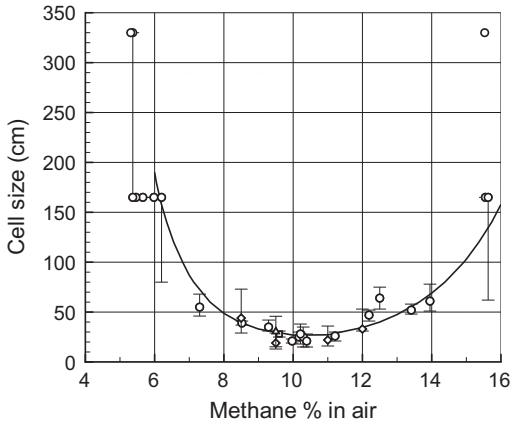

Fig. 10. Detonation cell sizes measured in GETF experiments (circles) and reported by Kuznetsov et al. [20] (diamonds), Tieszen et al. [14] (triangle) and Moen et al. [16] (square). Solid line shows computed cell size based on a model by Gavrikov et al. [24]. Points at 165 cm correspond to double-head spin detonations. Points at 330 cm correspond to single-head spin detonations.

These new detonability limits were determined using booster detonations in methane–oxygen mixture. In some experiments near the limits, the volume of the booster mixture was increased by a factor of two in order to avoid a possible detonation failure due to an insufficient initiation energy. The results are summarized in Fig. 15, where the initiation energy E (MJ/m^2) for GETF experiments was computed as $E = E_B V_B/S$, where E_B (MJ/m^3) is the energy released by the explosion of the stoichiometric mixture $CH_4 + 2O_2$ in the booster bag, V_B is the volume of the bag (see Table 1), and $S = 0.866$ m^2 is the tube cross-section. We assume $E_B = Q_{CH4}/3$, where $Q_{CH4} = 35.8$ MJ/m^3 is the heat of combustion of methane. The value of E computed here is based on the total chemical energy contained in the booster bag. We do not take into account the fact that the amount of energy actually involved in the detonation

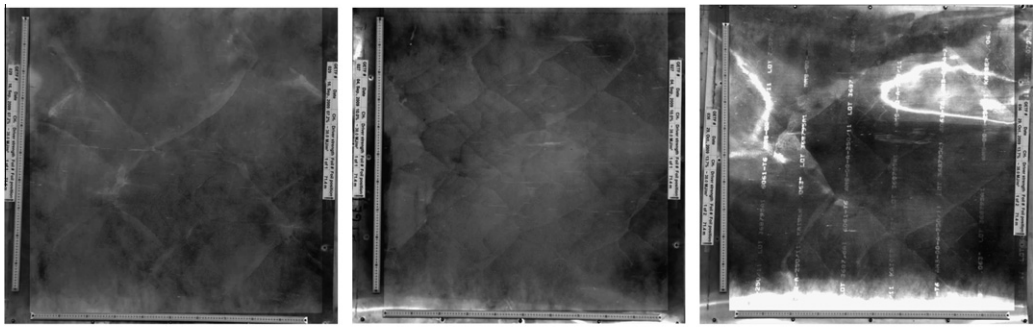

Fig. 11. Detonation cells on smoke foils: (a) Test #29, 7.2% NG. (b) Test #27, 10.2% NG. (c) Test #36, 13.7% NG. Full 1.2 m × 1.2 m foils are shown.

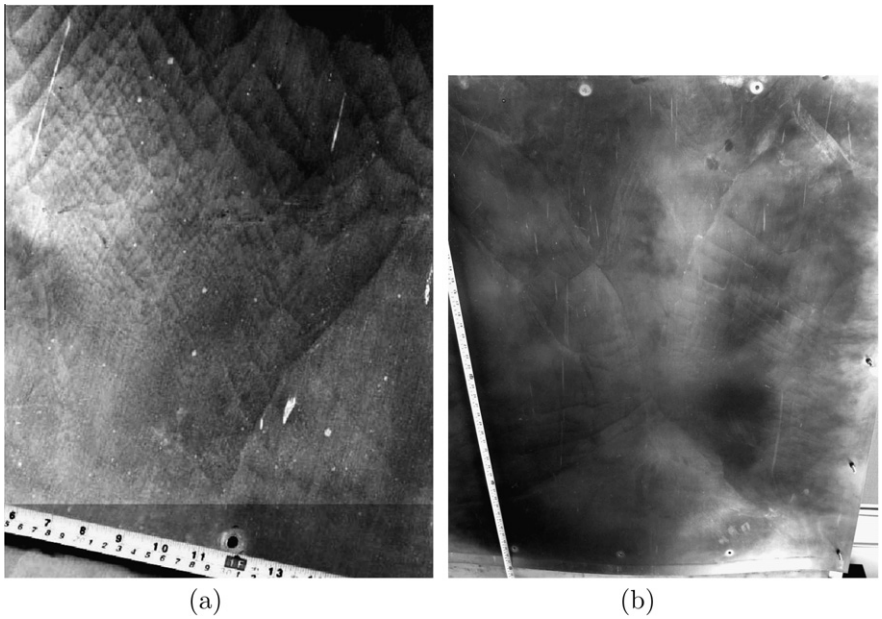

Fig. 12. Secondary detonation cells inside large main cell. (a) Test # 48, 6.2% NG. Scale is in inches (top) and centimeters (bottom). (b) Test #51, 5.5% NG. Foil height 1.2 m. Distance between mounting holes ~30 cm.

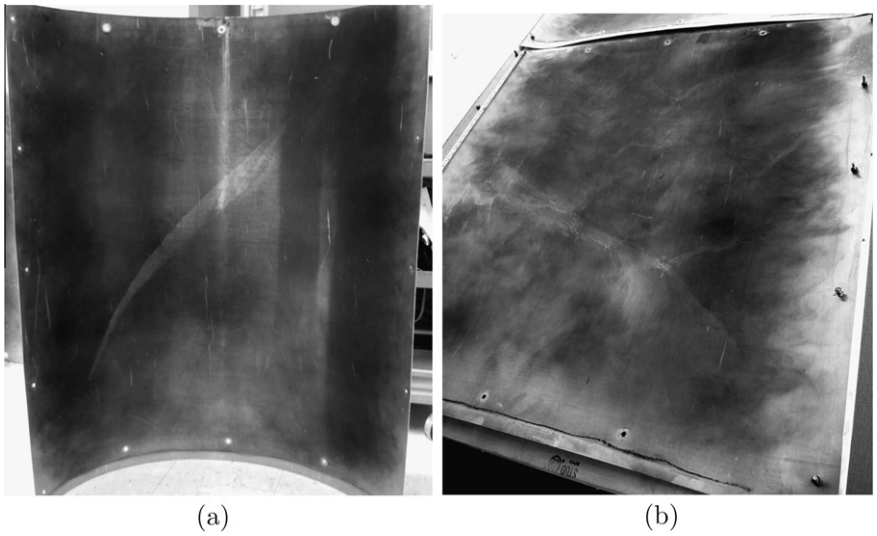

Fig. 13. Traces of spin detonations on smoke foils. (a) Test #57, 5.3% NG. (b) Test #49, 15.5% NG. Foil size 1.2 m × 1.2 m. Distance between mounting holes ~30 cm.

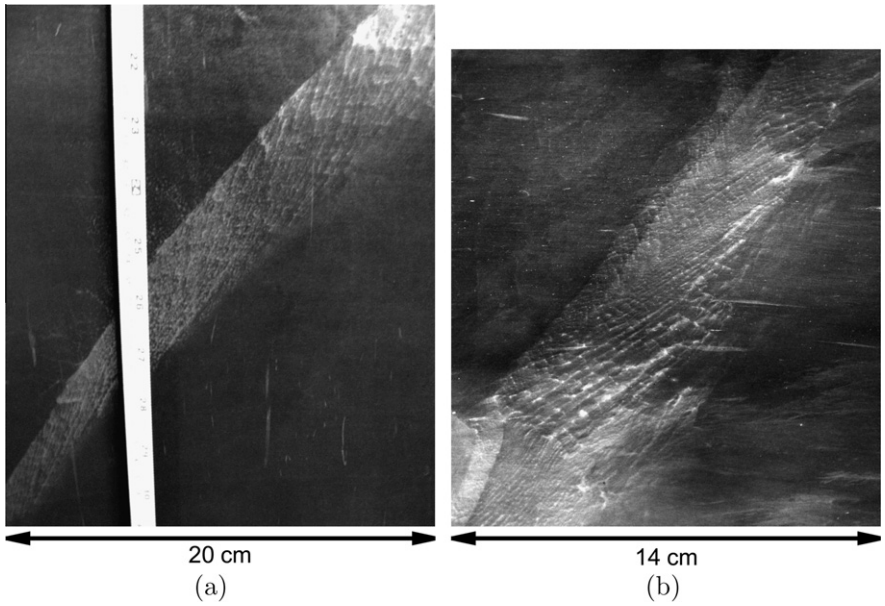

Fig. 14. Fine detonation cells inside spin detonation trace. (a) Test # 57, 5.3% NG. (b) Test #49, 15.5% NG.

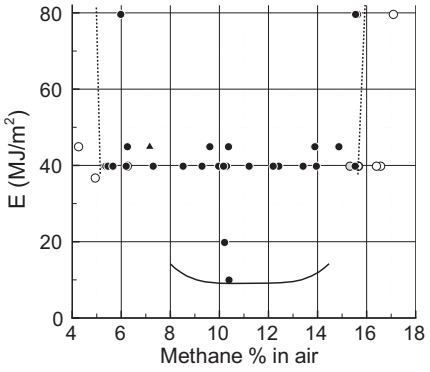

Fig. 15. Initiation energies provided by booster bags in GETF experiments (points). Point colors correspond to observed combustion regimes: detonations (black), deflagration (gray), no combustion (white). Triangle corresponds to DDT. Solid line shows minimum energy required for detonation initiation measured in Ref. [15].

initiation can be smaller than E and may not be proportional to V_B, since the detonation in the booster bag generates a shock with a decreasing pressure profile of a limited duration. It has been shown, for example, that the detonation initiation depends on the ratio between the transmitted shock pressure and the detonation pressure in the acceptor mixture [39]. The mechanism of initiation of a detonation in the acceptor mixture by a booster detonation can be quite complex, and is beyond the scope of this work.

Though systematic studies of the effect of ignition energy were not completed, the results presented in Fig. 15 show some influence of the initiation energy on the upper detonability limit. Figure 15 also shows that initiation energies used in GETF experiments are 4–8 times larger than minimum initiation energies measured in experiments [15] in a smaller tube. As the system approaches the detonability limits, the minimum energy required for the detonation initiation increases. For the wider limits observed in GETF experiments, the minimum energy may exceed the energy provided by the methane–oxygen booster. If this is the case, then true detonability limits in a 105-cm diameter tube can be slightly larger.

Figure 16 summarizes detonability limits measured for methane–air mixtures by different research groups in tubes of

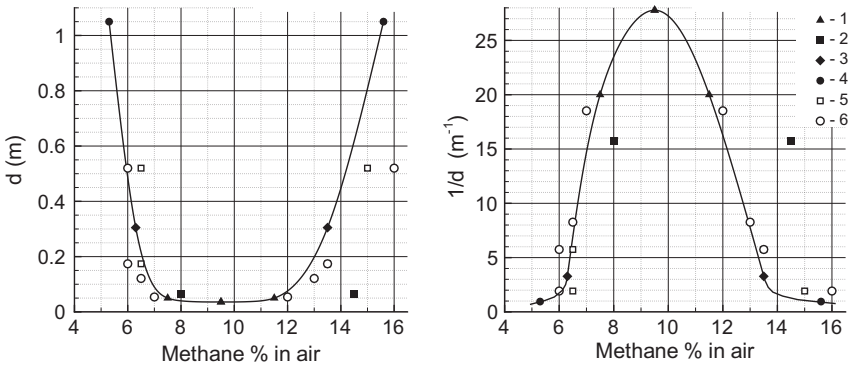

Fig. 16. Detonability limits measured for methane–air mixtures by different research groups in tubes of different diameters d (solid points): 1 – Matsui [21], 2 – Wolanski et al. [15], 3 – Kogarko [13], 4 – GETF. Solid line is the best fit for most of the experimental data. Open points show the boundary between subsonic and supersonic flames in methane–air mixtures in obstructed channels at 1 atm and 293 K: 5 – Kuznetsov et al. [22], 6 – Kuznetsov et al. [40]. Two plots show the same data in different coordinate systems.

different diameters d, and using different detonation initiation methods. Matsui [21] used a Schelkin spiral to produce DDT, Wolanski et al. [15] used hydrogen–oxygen booster, Kogarko [13] used a high explosive, and we used a methane–oxygen booster in GETF experiments.

The data are shown in Fig. 16 in two coordinate systems: d vs concentration and $1/d$ vs concentration. Most of the data fit on the U-shaped or bell-shaped curve depending on coordinates, that shows the wider detonability limits for larger systems. The limits defined in GETF experiments are the widest observed so far, but they are not the widest possible and should continue to grow with the system size.

Kuznetsov et al. [40,22] studied flame acceleration in obstructed channels filled with methane–air mixtures. Though detonations were not observed in these experiments, the boundary between subsonic and supersonic flames shown by open points in Fig. 16 is very close to the curve that represents detonability limits. This may imply that supersonic flames in obstructed channels partially rely on shock compression for an accelerated energy release. For mixtures that cannot detonate, the energy release does not accelerate enough in response to the shock compression, and therefore supersonic flames do not develop.

The widening detonability limits for larger systems can also be important for smaller systems at higher pressures. The effect of a larger scale is similar to the effect of a higher pressure, as recently shown in experiments [22] for concentration limits for flame acceleration and DDT. We therefore can expect wider detonability limits for methane–air mixtures used in engines that operate at increased pressures.

Acknowledgments

The authors thank Y. Sarrazin, S.B. Dorofeev, J.E. Shepherd, A.Yu. Starikovskiy, and F.R. Schauer for their invaluable suggestions for the design the GETF facility and experiments.

References

[1] L.J. Spadaccini, M.B. Colket III, Prog. Energy Combust. Sci. 20 (1994) 431–460.
[2] N. Lamoureux, C.-E. Paillard, Shock Waves 13 (2003) 57–68.
[3] A.G. Kim, The Composition of Coalbed Gas, Report of Investigation 7762, US Bureau of Mines, Washington, 1973.
[4] M.A. Trevits, G.L. Finfinger, Coalbed gas: an analysis of the relationship between gas content, gas composition and mine emissions, in: Proceedings of the 4th US Mine Ventilation Symposium, University of California, Berkley, CA, 1989.
[5] C.K. Westbrook, W.J. Pit, Combust. Sci. Technol. 33 (1983) 315–319.
[6] R. Vander Molen, J.A. Nicholls, Combust. Sci. Technol. 21 (1979) 75–78.
[7] J.A. Nicholls, M. Sichel, Z. Gabrijel, R.D. Oza, R. Vandermolen, Proc. Combust. Inst. 17 (1979) 1223–1234.
[8] S.M. Kogarko, V.V. Adushkin, A.G. Lyamin, Combust. Expl. Shock Waves 1 (1965) 15–22.
[9] D.C. Bull, J.E. Elsworth, G. Hooper, C.P. Quinnt, J. Phys. D: Appl. Phys. 9 (1976) 1991–2000.
[10] E.B. Vanta, J.C. Foster, G.H. Parsons, Detonability of Some Natural Gas–Air Mixtures, AFATL-TR-74-80, Air Force Armament Laboratory, Eglin. AFB, Florida, 1974.
[11] M.C. Parnarouskis, C.D. Lind, P.P.K. Raj, J.M. Cece, Vapor cloud explosion study, in: Proceedings of 6th International Conference on Liquefied Natural Gas, vol. 2, Session III, Kyoto, 1980, paper 12.
[12] W. Payman, W.C.F. Shepherd, Proc. R. Soc. London, A 158 (1937) 348–367.
[13] S.M. Kogarko, Soviet Phys. Tech. Phys. 3 (1959) 1904–1916.
[14] S.R. Tieszen, D.W. Stampsa, C.K. Westbrookb, W.J. Pitz, Combust. Flame 84 (1991) 376–390.
[15] P. Wolanski, C.W. Kauffman, M. Sichel, J.A. Nicholls, Proc. Combust. Inst. 18 (1981) 1651–1660.
[16] I.O. Moen, J.W. Funk, S.A. Ward, G.M. Rude, P.A. Thibault, Detonation length scales for fuel–air explosives, Prog. Astronaut. Aeronaut. 94 (1984) 55–79.
[17] M. Gerstein, E.D. Carlson, F.U. Hill, Indus. Eng. Chem. 46 (1954) 2558–2562.
[18] W. Bartknecht, Explosion, Springer-Verlag, Berlin, Germany, 1981.
[19] R.P. Lindstedt, H.J. Michels, Combust. Flame 76 (1989) 169–181.
[20] M. Kuznetsov, G. Ciccarelli, S. Dorofeev, V. Alekseev, Yu. Yankin, T.H. Kim, Shock Waves 12 (2002) 215–220.
[21] H. Matsui, J. de Physique IV 12 (2002). Pr7-11–Pr7-17.
[22] M. Kuznetsov, V. Alekseev, I. Matsukov, T.H. Kim, Ignition, flame acceleration and detonations of methane–air mixtures at different pressures and temperatures, in: Proceedings of 8th International Symposium on Hazards, Prevention, and Mitigation of Industrial Explosions, Yokohama, Japan, September 5–10, 2010, paper ISH-118.
[23] L. Fried, K. Glaesemann, P.C. Souers, W.M. Howard, P. Vitello, A Thermochemical-Kinetics Code CHEETAH 3.0, Lawrence Livermore National Laboratory, Livermore, CA, 2000.
[24] A.I. Gavrikov, A.A. Efimenko, S.B. Dorofeev, Combust. Flame 120 (2000) 19–33.
[25] V.I. Manzhalei, Fizika Goreniya i Vzryva 13 (1977) 470–472.
[26] V.N. Gamezo, A.M. Khokhlov, E.S. Oran, Secondary detonation cells in systems with high activation energy, in: Proceedings of the 17th ICDERS, 1999, paper 237.
[27] V.N. Gamezo, A.A. Vasil'ev, A.M. Khokhlov, E.S. Oran, Proc. Combust. Inst. 28 (2000) 611–617.
[28] H.N. Presles, D. Desbordes, M. Guirard, C. Guerraud, Shock Waves 6 (1996) 111–114.
[29] V.N. Gamezo, J.C. Wheeler, A.M. Khokhlov, E.S. Oran, Astrophys. J. 512 (1999) 827–842.
[30] F. Joubert, D. Desbordes, H.-N. Presles, Combust. Flame 152 (2008) 482–495.
[31] F. Virot, B. Khasainov, D. Desbordes, H.-N. Presles, Shock Waves 20 (2010) 457–465.
[32] A.A. Vasil'ev, V.A. Vasiliev, A.V. Trotsyuk, Combust. Expl. Shock Waves 46 (2010) 196–206.
[33] B.V. Voitsekhovski, V.V. Mitrofanov, M.E. Topchian, Proc. Combust. Inst. 12 (1969) 829–837.
[34] Yu.N. Denisov, Ya.K. Troshin, Doklady Akad. Nauk SSSR 125 (1959) 110–113.
[35] J.H. Lee, R.I. Soloukhin, A.K. Oppenheim, Astronaut. Acta 14 (1969) 565–584.
[36] V.I. Manzhalei, V.V. Mitrofanov, Fizika Gorenija i Vzryva 9 (1973) 703–710.
[37] D.A. Kessler, V.N. Gamezo, E.S. Oran, Proc. Combust. Inst. 33 (2011) 2211–2218.
[38] K.L. Cashdollar, I.A. Zlochower, G.M. Green, R.A. Thomas, M. Hertzberg, J. Loss Prev. Process. Ind. 13 (2000) 327–340.
[39] M.S. Kuznetsov, S.B. Dorofeev, A.A. Efimenko, V.I. Alekseev, W. Breitung, Shock Waves 7 (1997) 297–304.
[40] M. Kuznetsov, V. Alekseev, Yu. Yankin, S. Dorofeev, Combust. Sci. Technol. 174 (2002) 157–172.